Developmental Cell, Vol. 7, 571–583, October, 2004, Copyright ©2004 by Cell Press

Lamellipodin, an Ena/VASP Ligand, Is Implicated in the Regulation of Lamellipodial Dynamics

Matthias Krause,[1] Jonathan D. Leslie,[1] Mary Stewart,[1] Esther M. Lafuente,[2] Ferran Valderrama,[3] Radhika Jagannathan,[1] Geraldine A. Strasser,[1] Douglas A. Rubinson,[1] Hui Liu,[1] Michael Way,[3] Michael B. Yaffe,[1] Vassiliki A. Boussiotis,[2] and Frank B. Gertler[1,*]

[1]Department of Biology and
Center for Cancer Research
MIT
Cambridge, Massachusetts 02139

[2]Department of Medical Oncology
Dana-Farber Cancer Institute
Harvard Medical School
Boston, Massachusetts 02115

[3]Cell Motility Group
Cancer Research UK
Lincoln's Inn Fields Laboratories
London WC2A 3PX
United Kingdom

Summary

Lamellipodial protrusion is regulated by Ena/VASP proteins. We identified Lamellipodin (Lpd) as an Ena/VASP binding protein. Both proteins colocalize at the tips of lamellipodia and filopodia. Lpd is recruited to EPEC and *Vaccinia*, pathogens that exploit the actin cytoskeleton for their own motility. Lpd contains a PH domain that binds specifically to PI(3,4)P_2, an asymmetrically localized signal in chemotactic cells. Lpd's PH domain can localize to ruffles in PDGF-treated fibroblasts. Lpd overexpression increases lamellipodial protrusion velocity, an effect observed when Ena/VASP proteins are overexpressed or artificially targeted to the plasma membrane. Conversely, knockdown of Lpd expression impairs lamellipodia formation, reduces velocity of residual lamellipodial protrusion, and decreases F-actin content. These phenotypes are more severe than loss of Ena/VASP, suggesting that Lpd regulates other effectors of the actin cytoskeleton in addition to Ena/VASP.

Introduction

Directed cell motility is essential for animal development and physiology. Processes such as lymphocyte chemotaxis and axon guidance require changes in motility in response to environmental signals. Establishment of cell polarity is a prerequisite for these processes. Since chemotactic receptors are uniformly distributed, an intracellular event must initiate polarization (Servant et al., 1999). The first polarized molecules downstream of many chemotaxis receptors are phosphatidylinositol lipid products of PI-3 kinase, PI(3,4,5)P_3 and its metabolite PI(3,4)P_2 (Servant et al., 2000). These two 3′-phosphoinositides account for only 0.25% of all inositol-containing lipids, making them prime candidates for regulatory signaling molecules (Rameh and Cantley, 1999). Once polarity is established, rearrangement of the actin cytoskeleton provides the driving force for movement of the cell or growth cone up the chemotactic gradient. However, a direct connection between polarized phosphoinositides and proteins that remodel the actin cytoskeleton remains elusive.

In response to membrane-based signaling events, changes in actin dynamics are induced by a variety of actin-associated proteins including the Ena/VASP protein family. The Ena/VASP family includes three vertebrate members, Mena, VASP, and EVL (see review by Krause et al., 2003). They share a conserved domain structure: an N-terminal Ena/VASP homology 1 (EVH1) domain, a central proline-rich region, and a C-terminal Ena/VASP homology 2 (EVH2) domain. The EVH2 domain mediates tetramerization of Ena/VASP proteins through a coiled-coil motif and binds both G- and F-actin. The central proline-rich region harbors binding sites for SH3 and WW domain-containing proteins and for the G-actin binding protein Profilin. The EVH1 domain confers binding to proteins containing a specific proline-rich motif (D/E)(F/L/W/Y)PPPPX(D/E)(D/E) (abbreviated as FPPPP) (Niebuhr et al., 1997). This interaction is important for intracellular targeting of Ena/VASP proteins and for their recruitment to receptor/signaling complexes. For example, Ena/VASP proteins are targeted to focal adhesions through interaction with FPPPP motifs found in Zyxin and Vinculin (Drees et al., 2000; Gertler et al., 1996). FPPPP motifs are also found in the hematopoietic protein Fyb/SLAP/ADAP, the axon guidance receptor sax-3/Robo, and the ActA protein of the intracellular pathogen *Listeria monocytogenes* (Bashaw et al., 2000; Chakraborty et al., 1995; Krause et al., 2000).

In addition to their focal adhesion localization, Ena/VASP proteins localize to the tips of filopodia and lamellipodia (Lanier et al., 1999; Reinhard et al., 1992; Rottner et al., 1999). A GFP-EVH2 domain fusion localizes to lamellipodia in a broad pattern when expressed in fibroblasts (Loureiro et al., 2002). In contrast, a GFP-EVH1 domain construct localizes to the tip of lamellipodia (Bear et al., 2000). This led us to hypothesize that Ena/VASP proteins localize to filopodia and lamellipodila through combined function of the EVH1 and EVH2 domains and that the EVH1 domain restricts Ena/VASP localization to the tip. However, there were no known proteins containing EVH1 binding motifs that localize to the leading edge.

Leading edge localization is essential for Ena/VASP function in regulating random fibroblast motility. Ena/VASP proteins regulate the length and branching density of actin filaments. Overexpression or artificial targeting of Ena/VASP proteins to the leading edge leads to longer, less branched actin filaments. This results in faster protruding, but less stable, lamellipodia, which frequently form nonproductive ruffles. In contrast, lamellipodia that lack Ena/VASP protrude slowly but continue to extend for longer times. These steadier protrusions

*Correspondence: fgertler@mit.edu

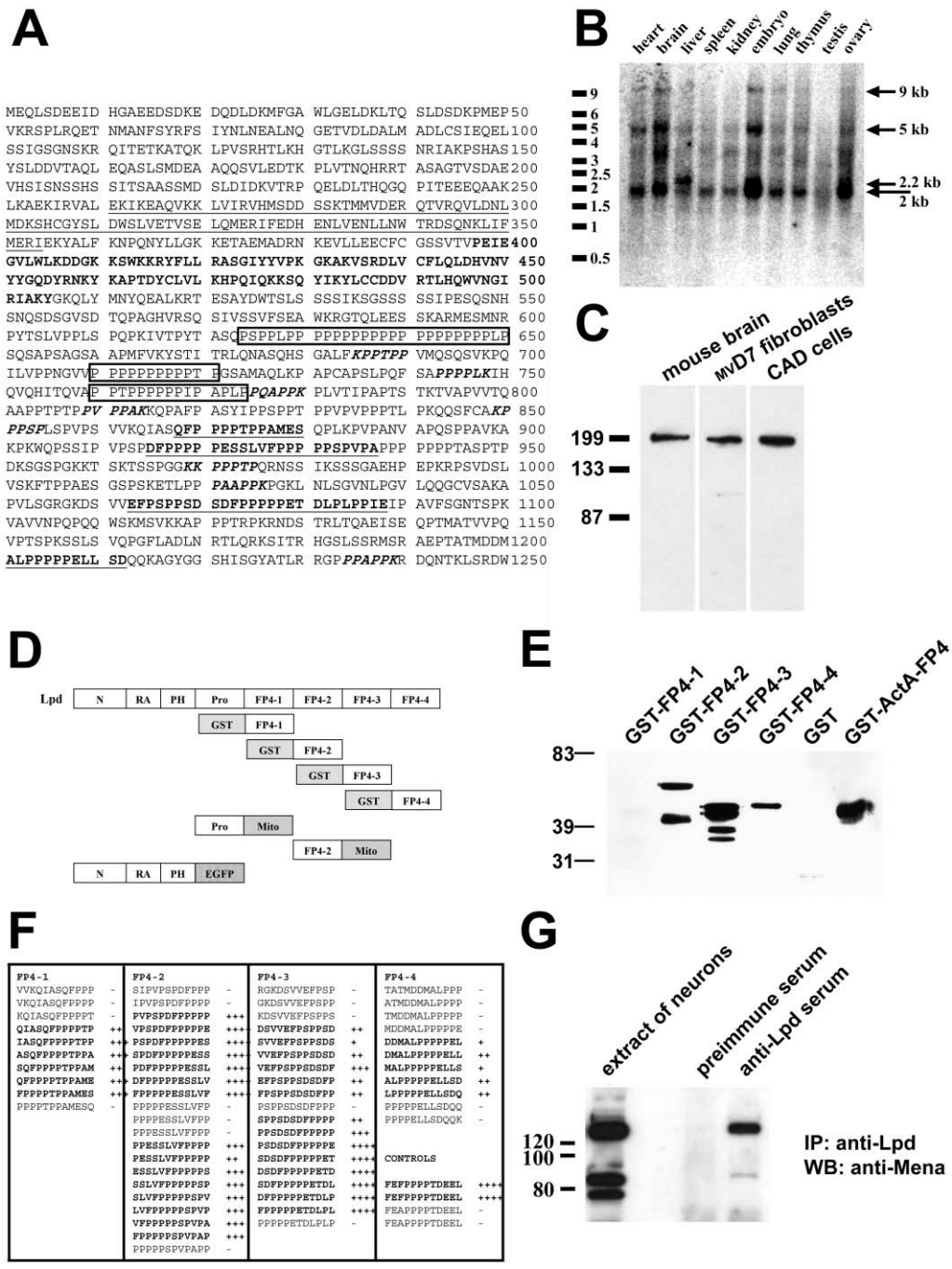

Figure 1. Lpd Is an Ena/VASP Binding Partner

(A) Amino acid sequence of Lpd. The RA domain (underlined), the PH domain (bold), eight SH3 binding sites (bold and italicized), three Profilin binding sites (boxed), and six EVH1 binding sites (bold and underlined) are shown.

(B) Lpd Northern blot. Arrows show Lpd mRNA at 2, 2.2, 5, and 9 kb.

(C) Immunodetection of Lpd in extracts of mouse brain, MV^{D7} fibroblasts, and CAD cells. The polyclonal Lpd antibody reacts specifically with a single band at approximately 200 kDa.

(D and E) Far Western blot analysis with purified, recombinant VASP on GST fusion proteins of Lpd. The location of GST-, Mito- (mitochondrial targeting anchor-), and EGFP-fusion proteins in Lpd is schematically indicated in (D). A GST fusion protein of the Ena/VASP binding sites in ActA serves as positive (GST-ActA-FP4) and GST as negative control. Bound VASP was detected with antibodies against VASP. Note that bands representing GST-fusion protein degradation products are visible.

(F) Peptide spot analysis of full-length Lpd. Peptides were synthesized on a cellulose membrane (SPOTS blot) and incubated with purified, recombinant EVL. Positive spots were detected with antibodies to EVL. Blots were scanned and intensity of positive spots quantified relative to the negative (ActA APPPP) and positive (ActA FPPPP) control.

(G) Coimmunoprecipitation of Lpd and Mena from primary cortical neurons. Extracts of primary cortical neurons were incubated with polyclonal antibodies to Lpd or preimmune serum as control. Immune complexes were collected using protein-A agarose, separated by SDS-PAGE, blotted, and probed with mAbs against Mena. Note that Mena is expressed in three isoforms of 80, 88, and 140 kDa in neurons.

result in faster net cell translocation rates of randomly migrating fibroblasts (Bear et al., 2002).

Here we report identification of Lamellipodin (Lpd), an EVH1 ligand of Ena/VASP proteins. Lpd colocalizes with Ena/VASP proteins exclusively at the tips of filopodia and lamellipodia. In addition, Lpd is recruited to EPEC and *Vaccinia* virus, pathogens that use the cellular signaling machinery to exploit the host actin cytoskeleton for their motility. Lpd's PH domain binds specifically to $PI(3,4)P_2$ and is sufficient for plasma membrane recruitment upon treatment with PDGF. Lpd overexpression produces faster lamellipodial protrusions similar to those observed when Ena/VASP is overexpressed or artificially targeted to the plasma membrane. In contrast, knockdown of Lpd expression results in impairment of lamellipodia formation, a phenotype more severe than that caused by loss of all Ena/VASP proteins. We propose a model in which Lpd cooperates with Ena/VASP proteins and other regulators of actin cytoskeleton to transduce signals from chemotaxis receptors into cytoskeletal dynamics.

Results

Identification of Lpd as an EVH1 Ligand

To identify EVH1 ligands, we screened public databases for proteins harboring FPPPP motifs. Several candidate proteins were identified. One human cDNA, KIAA1681, was chosen for further characterization based on the presence of a pleckstrin homology (PH) domain, raising the possibility that it may localize to the plasma membrane. Furthermore, KIAA1681 is a mammalian ortholog of *C. elegans mig-10*, a gene identified in a screen for neuronal cell migration defects (Manser et al., 1997). We named KIAA1681 Lamellipodin (Lpd), since it localized to the tips of lamellipodia and filopodia (see below).

Domain Structure and Isoforms of Lpd

The N terminus of Lpd (aa 1–50) is highly charged and is followed by a putative coiled-coil motif, Ras-association (RA), and PH domains. The C terminus is proline-rich, harboring eight potential SH3 binding sites, three potential Profilin binding sites, and four clusters containing a total of six putative EVH1 binding sites (Figure 1A).

During our analysis of Lpd, a related mammalian protein called RIAM (Rap1 interacting adaptor molecule) appeared in the database, revealing that Lpd belongs to a family of proteins (see accompanying article by Lafuente et al. [2004]). Both proteins share conserved RA and PH domains followed by a more divergent proline-rich C terminus (23.2% amino acid identity). Both C termini contain putative binding sites for EVH1 domains, SH3 domains, and Profilin. However, the C terminus of Lpd is 500 amino acids longer than RIAM's. The two proteins also differ at their N termini (29.1% amino acid identity), with RIAM harboring two additional putative EVH1 binding sites and one additional potential coiled-coil domain.

Database analysis also revealed that Lpd has at least one splice isoform, an uncharacterized cDNA termed ALS2CR9. This cDNA was originally cloned as one of 42 genes in the genomic region responsible for amyotrophic lateral sclerosis 2 (ALS2). However, mutations in ALS2CR9 are not responsible for ALS2 (Hadano et al., 2001). Therefore, we propose to rename ALS2CR9 as Lamellipodin-S (for "short;" Lpd-S). Northern blot analysis with a probe encoding part of the N terminus identified three broadly expressed Lpd isoforms of approximately 9, 5, and 2 kb. Lpd is most highly expressed in brain, heart, ovary, and developing embryo. An additional 2.2 kb isoform is expressed in embryo, ovary, and liver (Figure 1B). EST data and gene prediction programs suggest that the 5 kb and 9 kb bands code for Lpd cDNAs with 3′ UTRs of varying length. The 2 and 2.2 kb species may represent shorter splice variants, including Lpd-S.

We raised and affinity purified rabbit polyclonal antibodies against the Lpd C terminus. These antibodies recognize a single 200 kDa band in Western blots of cell and mouse brain extracts (Figure 1C). This suggests that the shorter splice variants lack the C terminus and are not recognized by the antibody. In vitro translation of the Lpd cDNA also produced a 200 kDa band, indicating that this cDNA represents full-length protein (data not shown).

Lpd Binds Ena/VASP Proteins In Vitro and In Vivo

Since Lpd harbors four clusters of putative EVH1 binding sites, we tested whether Lpd binds VASP directly. We purified four GST-fusion proteins, each containing one of the clusters of potential EVH1 binding sites (Figure 1D). The fusion proteins were blotted and overlaid with purified recombinant VASP in a far Western assay. A GST-fusion protein containing the known EVH1 binding sites from *Listeria* ActA served as the positive control and GST alone as the negative control. VASP bound to the second, third, and fourth Lpd GST-fusion proteins but not to the first, providing evidence that VASP can bind Lpd directly (Figure 1E).

To clarify which putative EVH1 binding sites within Lpd bind Ena/VASP, we used EVL to probe a SPOTS blot of individual EVH1 binding sites. A SPOTS blot contains a series of peptides synthesized directly on a membrane as individual spots. All six potential EVH1 binding sites in Lpd showed medium to strong binding to EVL when compared to the EVH1 binding site from *Listeria* ActA (Figure 1F). This indicates that all six sites can bind the EVH1 domain of Ena/VASP proteins. In light of this data, the failure of the first site to interact in the far Western assay could represent misfolding of this GST-fusion protein.

To determine whether Ena/VASP and Lpd associate in cells, we used anti-Lpd antibodies to immunoprecipitate Lpd from lysates of 293 cells overexpressing both GFP-Lpd and mRFP-EVL. We found that mRFP-EVL coimmunoprecipitated with GFP-Lpd from these lysates (data not shown). Since Lpd and Mena are most highly expressed in the nervous system, we repeated the immunoprecipitation with endogenous protein using extracts of cultured primary cortical neurons. We were able to coimmunoprecipitate Mena with Lpd (Figure 1G). Therefore, endogenous Lpd and Ena/VASP proteins are present in protein complexes in vivo.

Lpd Colocalizes with Ena/VASP Proteins at the Tips of Lamellipodia and Filopodia

We used affinity-purified polyclonal antibodies to analyze Lpd's localization in cultured cells. In Rat2 fibroblasts, WI-38 human lung fibroblasts, and B16-F1

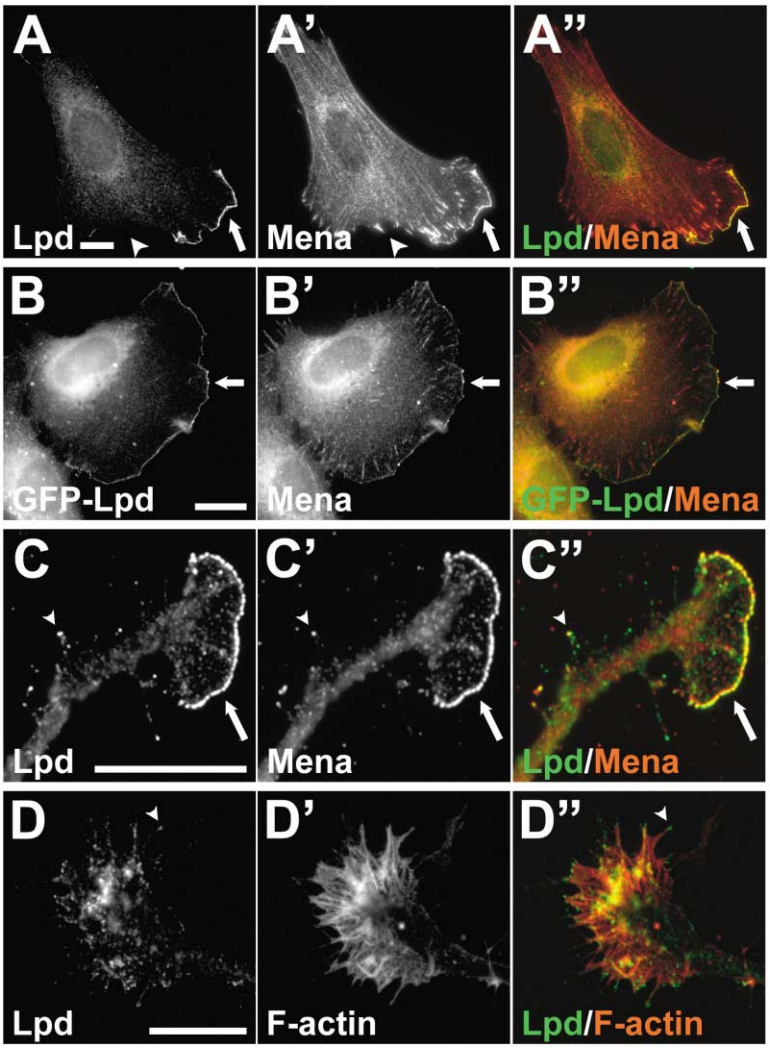

Figure 2. Lpd Colocalizes with Ena/VASP Proteins at the Tips of Filopodia and Lamellipodia

(A and C) Rat2 cells (A–A″) and CAD cells (C–C″) were cultured on glass coverslips, fixed, and double stained for Lpd (A and C) and Mena (A′ and C′).

(D) Primary hippocampal neurons (D–D″) were double stained for Lpd (D) and F-actin (D′). Lpd is localized at the tips of filopodia (arrowhead in C and D).

(B–B″) Rat2 cells, stably expressing GFP-Lpd (B) were stained for Mena (B′).

Colocalization between Lpd and Mena is observed in the merged images at the tips of lamellipodia (arrow in A″, B″, and C″) and filopodia (arrowheads in C–C″). Scale bars in (A)–(D) (for first two panels of each row) equal 15 μm.

mouse melanoma cells, Lpd was concentrated at the tips of lamellipodia and filopodia and colocalized with Ena/VASP proteins (arrow in Figures 2A–2A″ and 4C–4C″ and not shown). Unlike two other known FPPPP-containing proteins, Zyxin and Vinculin, Lpd was not detected in focal adhesions (arrowhead in Figures 2A and 2A′). Consistent with the immunolocalization, EGFP-tagged full-length Lpd colocalized with endogenous Mena at the tips of filopodia and lamellipodia in Rat2 fibroblasts (arrow in Figures 2B–2B″). In the growth cone-like structures of differentiated CAD cells, a murine neuronal cell line, Lpd also colocalized with Ena/VASP proteins at the distal tips of lamellipodia and filopodia (arrow and arrowhead, respectively, in Figures 2C–2C″). Similarly, in primary growth cones, Lpd was found at the tips of filopodia (arrowhead in Figures 2D–2D″) and in spots along the axon shaft.

Lpd Colocalizes with *Vaccinia* Virus and EPEC but Not *Shigella* and *Listeria*

A variety of pathogens exploit the host actin cytoskeleton in different ways for their own motility. Several host cytoskeletal proteins associate with these pathogens and have been implicated in F-actin dynamics (Frischknecht and Way, 2001; Gruenheid and Finlay, 2003). We sought to determine if such pathogens could recruit Lpd by staining infected cells with the anti-Lpd antibody.

Both *Listeria monocytogenes* and *Shigella flexneri* invade mammalian cells and use the actin cytoskeleton to propel them through the cytoplasm on top of F-actin tails (Cossart, 2000). Lpd is not recruited to the interface between *Listeria* or *Shigella* and their F-actin tails (Figures 3C and 3D).

Vaccinia infects cells, multiplies, and is then transported on microtubules to the plasma membrane as an enveloped virus (Smith et al., 2002). After membrane fusion, the extracellular virus induces an intracellular actin tail that propels it along the surface of the plasma membrane (Rietdorf et al., 2001). Interestingly, Lpd localized to the interface between *Vaccinia* and its actin tail (arrow in Figure 3A).

Enteropathogenic E. coli (EPEC) does not invade the host cell, but instead docks on the outer membrane surface and injects bacterial proteins into its host. This results in the formation of "actin pedestals" underneath

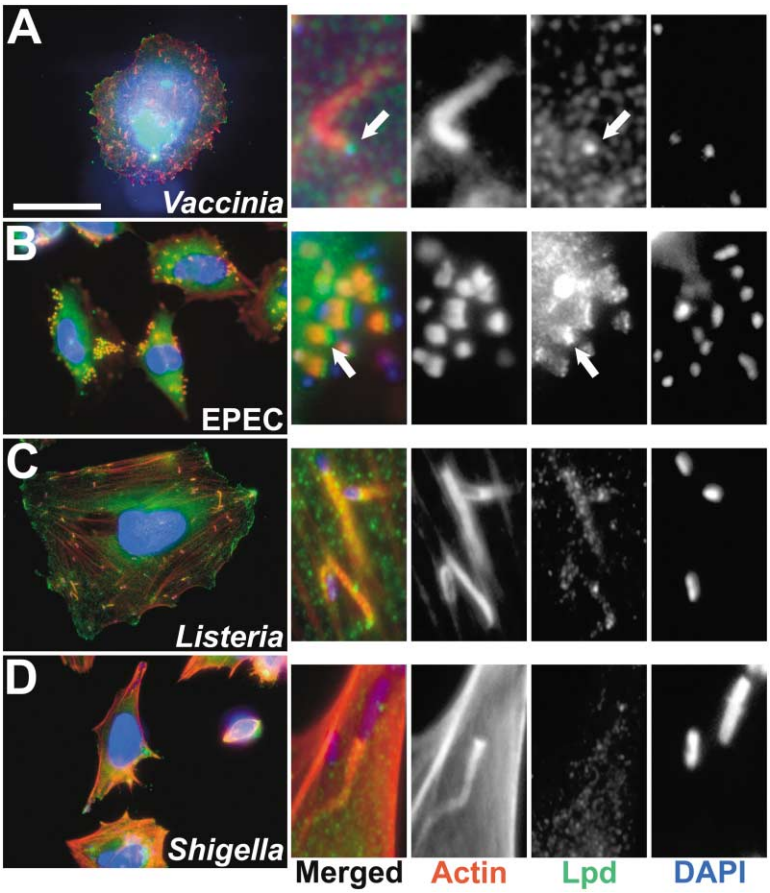

Figure 3. Lpd Localizes to *Vaccinia* and EPEC but Not *Listeria* and *Shigella*

HeLa cells were infected with (A) *Vaccinia* virus, (B) *Enteropathogenic E. coli* (EPEC), (C) *Listeria monocytogenes*, and (D) *Shigella flexneri*. After fixation, cells were stained with anti-Lpd antibodies and specific, dye-labeled probes for F-actin (phalloidin) and DNA (DAPI stain). High-magnification insets show localization of Lpd (arrows in [A] and [B]) at the interface between *Vaccinia* or EPEC and the respective F-actin-rich structure. Scale bar in (A) for (A)–(D) equals 20 μm.

the attached bacteria (Celli et al., 2000). Lpd was recruited to the interface between EPEC and their actin pedestals (arrow in Figure 3B).

Lpd Localization Is Independent of Ena/VASP Proteins

MV^{D7} cells lack all three Ena/VASP proteins (Bear et al., 2000). Lpd localization in this cell line was indistinguishable from cells expressing Ena/VASP proteins (Figure 4A). Ena/VASP localization at the leading edge requires both the EVH1 domain and association of the EVH2 domain with free barbed ends of actin filaments. Exposure of cells to low doses (150 nM) of cytochalasin D (CD) blocks free barbed ends and displaces Ena/VASP proteins from the leading edge of cells (Bear et al., 2002). Lpd localization was unaffected by the same CD treatment (Figures 4B–4B″). Control cells treated with DMSO, the solvent for CD, showed normal colocalization of Mena and Lpd (Figures 4C–4C″). Therefore, leading edge localization of Lpd is independent of Ena/VASP proteins and free F-actin barbed ends.

Since Lpd localizes independently of Ena/VASP proteins and can bind to them in vivo, we wondered whether Lpd could direct Ena/VASP localization. To test this hypothesis, we targeted parts of Lpd to mitochondria by fusing them to a mitochondrial membrane anchor (Bear et al., 2000). Expression of the second cluster of Ena/VASP binding sites (Lpd-FP4-2-Mito, see Figure 1D) caused Mena to relocalize to the mitochondrial surface (Figures 4D–4D″). A proline-rich region of Lpd that does not contain EVH1 binding sites (Lpd-Pro-Mito) did not cause Mena relocalization (Figures 4E–4E″). Therefore, the EVH1 binding motifs within Lpd can recruit Ena/VASP proteins to specific sites within living cells.

The Lpd PH Domain Is Specific for PI(3,4)P_2 and Sufficient for Leading Edge Targeting upon PDGF Stimulation

To delineate the region of Lpd required for its leading edge localization, we expressed the N terminus of Lpd encompassing the RA and PH domains as an EGFP fusion (N-RA-PH-EGFP, see Figure 1D). N-RA-PH-EGFP localized to the leading edge in a pattern identical to full-length Lpd (Figures 5A–5A″). A smaller fragment containing just the RA and PH domains also localized to the leading edge (data not shown). Therefore, the RA and PH domains together are sufficient for leading edge targeting.

PH domains are phospholipid binding modules that can target proteins to the inner leaflet of the plasma membrane (Fruman et al., 1999). PH domains often possess specificity for certain phosphoinositides, and various signaling pathways can lead to enrichment or depletion of specific phosphoinositides in different membrane compartments. We tested the specificity of the Lpd PH domain in a lipid binding assay in which individual phospholipids were spotted on a membrane and then overlaid with GST-fusion proteins (Dowler et al., 2002; Kanai et al., 2001). A GST-Lpd PH domain fusion protein bound specifically to PI(3,4)P_2. The PX domain of P40 phox, a

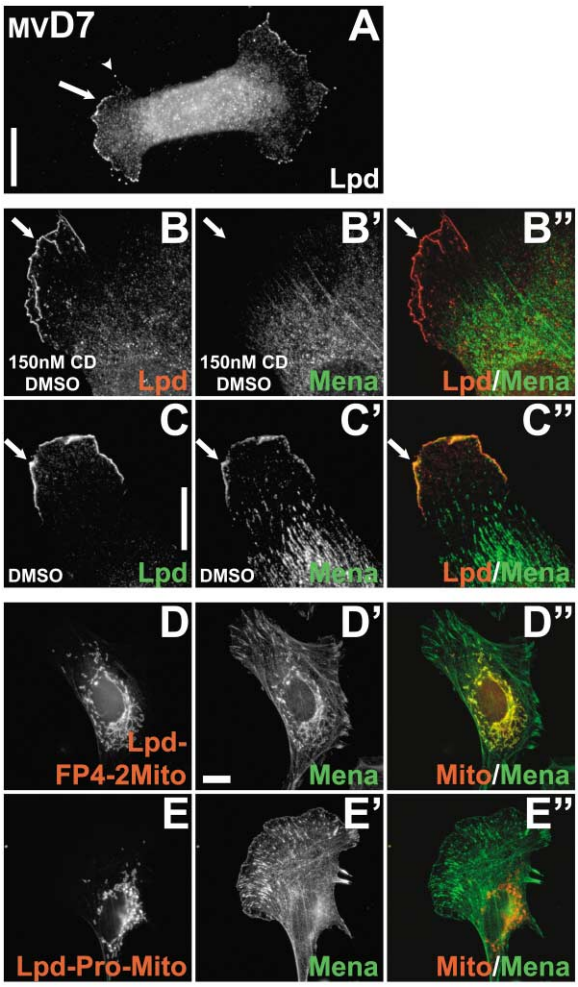

Figure 4. Lpd Localizes Independently of Ena/VASP Proteins to the Leading Edge and Can Recruit Ena/VASP Proteins to Specific Sites within the Cell

(A) The Ena/VASP-deficient cell line MV^{D7} was fixed and stained with anti-Lpd antibodies. Lpd localizes to the tips of filopodia (arrowhead) and lamellipodia (arrow).

(B and C) WI-38 lung fibroblasts treated with either 150 nM Cytochalasin D (CD) in DMSO (B–B″) or with DMSO only (C–C″) were fixed and costained with antibodies against Lpd (B and C) and Mena (B′ and C′). Merged images of (B) and (B′) or (C) and (C′) are shown in (B″) and (C″), respectively. Note that Mena but not Lpd is delocalized by treatment with CD (arrows).

(D and E) Lpd can recruit Ena/VASP proteins to specific sites within cells. The second cluster of the EVH1 binding sites in Lpd (Lpd-Fp4-2Mito) (D–D″) or the proline-rich region behind the PH domain of Lpd (Lpd-Pro-Mito) (E–E″) was fused to DSred2 as a marker and to a mitochondrial membrane anchor (see Figure 1D for location of fragments in Lpd). Stably transfected Rat2 fibroblasts were fixed and stained with anti-Mena antibodies (D′ and E′). Mena is only corecruited to mitochondria by the Lpd-FP4-2 fragment (yellow color in D″).

Scale bars in (A), (C) (for all [B] and [C] panels), and (D′) (for all [D] and [E] panels) equal 15 μm.

phosphoinositide binding domain specific for PI(3)P, was used as a positive control and GST alone as the negative control (Figure 5B).

The association of the Lpd PH domain with $PI(3,4)P_2$ was verified in an ultracentrifugation assay for liposome (lipid-vesicle) binding. Proteins were tested for their ability to interact with liposomes composed of phosphatidyl choline (PC), phosphatidyl ethanolamine (PE), with or without $PI(3,4)P_2$. The PX domain of P47phox, known to bind specifically to $PI(3,4)P_2$ (Kanai et al., 2001), bound to PC/PE/$PI(3,4)P_2$ liposomes as expected. The PH domain of Lpd bound to PC/PE liposomes containing $PI(3,4)P_2$ (two independent experiments: 15% and 23% binding) but did not bind to control PC/PE liposomes (0% binding).

Quiescent fibroblasts stimulated with PDGF react with immediate $PI(3,4)P_2$ production and ruffle formation (Rameh and Cantley, 1999). To test the hypothesis that $PI(3,4)P_2$ recruits the PH domain of Lpd to the plasma membrane, we expressed the PH domain of Lpd as an EGFP fusion (EGFP-PH) in Rat2 fibroblasts. Cells were serum starved and then treated with PDGF to induce ruffling. The EGFP-PH construct was recruited to PDGF-induced membrane ruffles, where it colocalized with endogenous Mena (Figures 5C–5C″).

Lpd Overexpression in Fibroblast Increases Lamellipodial Protrusion Velocity

To evaluate Lpd function during lamellipodia formation, we analyzed the behavior of lamellipodia over time by kymography (Hinz et al., 1999). Within the kymograph, the slope of a protrusion represents lamellipodial extension velocity.

We first examined the effect of Lpd overexpression on nascent lamellipodia. To synchronize the activation state of cells, we analyzed fibroblasts recovering from azide treatment (Svitkina et al., 1986). Treatment of cells with sodium azide in the absence of glucose causes rapid depletion of intracellular ATP, causing actin filament depolymerization and cell retraction. Upon azide washout and restoration of glucose, cells respond with synchronized protrusions of circumferential lamellipodia.

Under these conditions, wild-type Rat2 fibroblasts extend slow wave-like protrusions (Figures 6A and 6B). In contrast, Rat2 fibroblasts stably overexpressing EGFP-Lpd to roughly double the normal expression level (Figure 2B and not shown) formed faster protrusions that frequently turned into ruffles (Figures 6C and 6D). Quantification revealed that lamellipodia of Lpd-overexpressing cells protruded with significantly faster velocity than wild-type Rat2 fibroblasts (Figure 6E). A similar phenotype was also observed when cells were analyzed under steady-state conditions without azide treatment (Figure 6F). Importantly, the Lpd overexpression phenotype resembles the effects of Ena/VASP overexpression or artificial targeting of Ena/VASP to the plasma membrane (Bear et al., 2002).

To test whether the Lpd overexpression phenotype is dependent on Ena/VASP proteins, we neutralized Ena/VASP function in the Lpd-overexpressing Rat2 fibroblasts and control, wild-type Rat2 cells. We used a strategy to deplete all Ena/VASP proteins from their normal intracellular locations by expressing the EVH1 binding sites from ActA fused to a mitochondrial membrane anchor (FPPPP-Mito), thereby artificially recruiting Ena/VASP proteins to mitochondria (Bear et al., 2000). Rat2 fibroblasts in which Ena/VASP function had been blocked

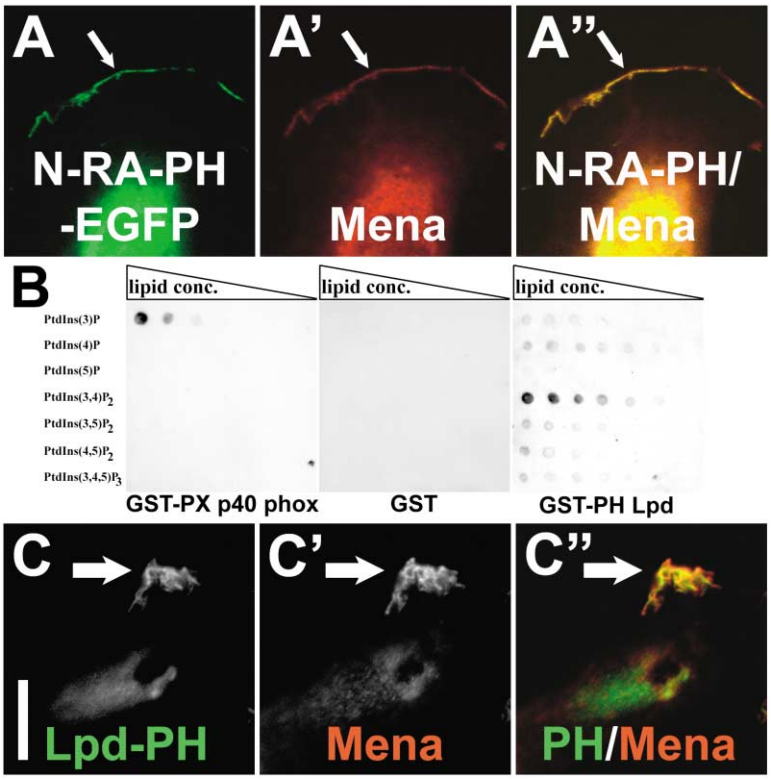

Figure 5. Lpd's PH Domain Binds to PI(3,4)P_2 and Is Sufficient for Leading Edge Targeting upon PDGF Treatment of Serum-Starved Fibroblasts

(A) An EGFP-fusion protein with the N terminus of Lpd including the RA and PH domain was stably expressed in Rat2 fibroblasts. After fixation, cells were stained with anti-Mena antibodies (arrow in A′). Note that EGFP-N-term-RA-PH localizes to the leading edge (arrow in A). (A″) Colocalization between the EGFP fusion protein and Mena is observed in the merged images at the tips of lamellipodia (arrow in A″).

(B) A protein-lipid binding assay was used to analyze the ability of purified GST-fusion proteins to bind a variety of phosphoinositides. Serial dilutions of the indicated phosphoinositides (200, 100, 50, 25, 12.5, and 6.25 pmol) were spotted on to HybondC-membranes and incubated with GST-fusion proteins. After washing the membranes, bound proteins were detected with anti-GST antibodies. The PX domain of p40phox served as the positive control (specific for PI(3)P) and GST alone as negative control. The PH domain of Lpd binds specifically only to PI(3,4)P_2.

(C) The localization of an EGFP-fusion protein with the PH domain of Lpd (EGFP-Lpd-PH) was tested in PDGF-stimulated Rat2 fibroblasts. Rat2 cells, stably expressing EGFP-Lpd-PH, were serum starved, treated with PDGF, fixed, and stained with anti-Mena antibodies. EGFP-Lpd-PH is recruited to PDGF-induced ruffles were it colocalizes with Mena (arrows). Scale bar in (C) (for A and C) equals 15 μm.

extended lamellipodia with a significantly reduced velocity compared to wild-type Rat2 cells or Rat2 cells expressing a control construct (APPPP-mito) that does not bind to Ena/VASP proteins (Bear et al., 2000). Expression of FPPPP-mito in Lpd-overexpressing Rat2 reduced the velocity of lamellipodial protrusions significantly (Figure 6F). Therefore, the effect of Lpd overexpression on lamellipodial protrusion velocity can be suppressed by blocking Ena/VASP function.

Knockdown of Lpd Expression Impairs Lamellipodia Formation

We used lentiviral-mediated expression of a Lpd-specific shRNA to stably knockdown Lpd expression. We analyzed B16-F1 mouse melanoma cells, as these cells do not express the related RIAM protein (data not shown). As a negative control, we used a shRNA directed against the corresponding rat Lpd sequence, which differs in several base pairs. The Lpd knockdown cell line (Lpd-KD) showed highly reduced expression of Lpd compared to a control cell line expressing the rat Lpd shRNA (control) (Figure 7E). When plated on laminin, B16-F1 cells form large lamellipodia that can be labeled with an antibody against N-WASP. Strikingly, Lpd-KD cells formed very few lamellipodia (Figures 7A and 7A′). Quantification of the ratio between the perimeter of lamellipodium to total perimeter of the cell revealed that reduction in Lpd expression reduced lamellipodia formation significantly (Figure 7A″). This was accompanied by a decrease in total area of the Lpd-KD cells (not shown). Analysis of the dynamics of the residual lamellipodia in the Lpd-KD cell line by kymography showed that these lamellipodia protruded with a significantly lower velocity than control (Figures 7B–7D).

Actin polymerization directly underneath the plasma membrane provides the driving force for lamellipodial protrusion. We fixed and stained the Lpd-KD and control cell lines with fluorescently labeled phalloidin to analyze the integrity of the actin cytoskeleton. Interestingly, the F-actin content of the Lpd-KD cell line appeared highly reduced (Figures 7F and 7G). Quantification by spectrofluorometry revealed that total F-actin content in Lpd-KD cells was indeed reduced compared to control (two independent assays in triplicate: reduced by 26.8% ± 14.6% compared to control). However, total actin content appeared to be comparable in knockdown and control cell lines as judged by Western blot analysis (Figure 7E). This suggests that the ratio of F- to G-actin is reduced in the Lpd knockdown cells. We used platinum replica electron microscopy to analyze the underlying actin ultrastructure in more detail. A thin rim of normal dense meshwork of actin filaments was visible directly underneath the plasma membrane of Lpd-KD cells; however, large areas deeper inside the cell periphery contained only thick bundles of F-actin and were devoid of a dense F-actin meshwork. In contrast, the control cell line showed a dense actin filament meshwork throughout the cell periphery (Figures 7H and 7I and enlarged areas in 7H′ and 7I′).

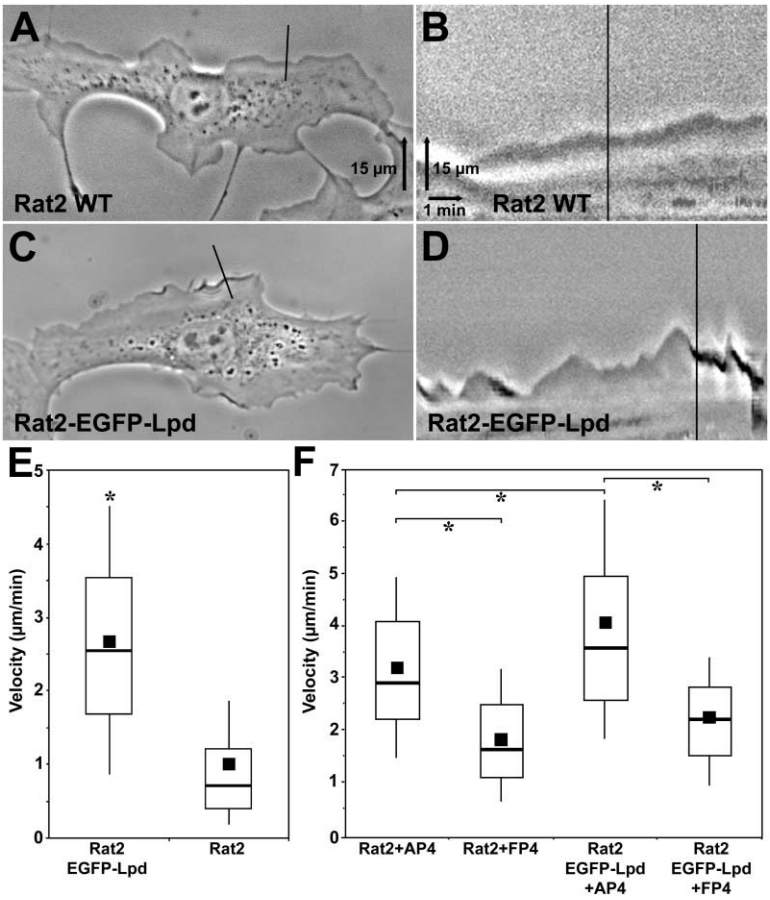

Figure 6. Kymograph Analysis of Rat2 Cells Overexpressing EGFP-Lpd

(A–D) Time-lapse movies of Rat2 cells (A and B) and Rat2 cells overexpressing EGFP-Lpd (C and D) recovering from ATP starvation were analyzed by drawing a one pixel wide line at a 90° angle across a lamellipodium in the direction of protrusion (line in individual frame of movie in [A] and [C]). The image from this line was copied from each frame of a movie and pasted along the x axis to generate a composite kymograhic image (B and D). The black line in (B) and (D) indicates the location of frames in kymographs. Within the kymograph, a steeper slope of a protrusion corresponds to higher velocity rates for lamellipodia protrusion. Scale bar for (A) and (C) and scale vectors for (B) and (D) are shown in top images.

(E) Box and whisker plots for velocity of individual nacsent protrusion events in wild-type and EGFP-Lpd overexpressing Rat2 cells recovering from ATP starvation. Top and bottom of box represent 75th and 25th quartile, and whiskers 10th and 90th percentiles, respectively. Dot indicates mean and middle line of box median. Data for wild-type cells is from 570 and for EGFP-Lpd overexpressing Rat2 cells from 934 protrusion events. Asterisk indicates significant difference in Student's t test ($p < 0.001$).

(F) Box and whisker plots for velocity of individual protrusions from cells under steady-state conditions. Rat2 cells expressing APPPP-Mito (control) or FPPPP-Mito (to block Ena/VASP function) alone or along with Lpd overexpression are shown. Brackets with asterisks indicate statistically significant differences between data sets using ANOVA ($p < 0.005$).

Discussion

Based on our results, we propose that Lpd acts as a convergence point between upstream signaling pathways and cytoskeletal remodeling at the plasma membrane. This hypothesis is supported by the recruitment of Lpd to two pathogens, EPEC and *Vaccinia*, that exploit cellular signaling processes at the plasma membrane to reorganize the actin cytoskeleton for their own motility. Furthermore, Lpd is concentrated at the tip of growth cone filopodia, a structure that plays a key role in guidance signal detection and growth cone motility. Lpd is likely to receive signals directly from both phosphoinositides through its PH domain and Ras superfamily proteins through its RA domain. The Lpd PH domain selectively binds PI(3,4)P_2, a phosphoinositide associated with polarization signals in a variety of cell types.

One way that Lpd is linked to cytoskeletal dynamics is through Ena/VASP proteins. Lpd associates with Ena/VASP by direct binding and can be detected in protein complexes from primary neurons. Ena/VASP and Lpd colocalize in filopodia and lamellipodial tips, and both types of proteins play critical roles in regulating lamellipodial dynamics. Lpd overexpression induces an increase in lamellipodial ruffling, similar to phenotypes that are observed when Ena/VASP activity is elevated in mammalian cells, and the Lpd overexpression phenotype requires Ena/VASP function. Interestingly, knockdown of Lpd led to impairment of lamellipodia formation, a phenotype not observed in cells devoid of all Ena/VASP proteins. This suggests that Lpd signals to other regulators of the actin cytoskeleton in addition to Ena/VASP proteins.

Lpd Contains High-Affinity Binding Sites for the EVH1 Domain of Ena/VASP

The EVH1 binding sites within Lpd match the canonical motif for EVH1 binding, found in the *Listeria monocytogenes* protein ActA. Two of the motifs in Lpd contain a phenylalanine followed by four consecutive prolines, flanking acidic amino acids, and a leucine in position 13 ($D_1S_2D_3F_4P_5P_6P_7P_8P_9E_{10}T_{11}D_{12}L_{13}$). This combination has been shown to have a high binding affinity for EVH1 domains and has not been found in any other mammalian EVH1 ligand (Ball et al., 2000; Niebuhr et al., 1997). Furthermore, Lpd and RIAM, with a total of 6 EVH1 binding sites each, contain the largest number of EVH1 binding sites of any known protein.

Lpd Localizes to the Tips of Lamellipodia and Filopodia

Lpd and Ena/VASP proteins colocalize in migrating cells at the tips of lamellipodia and filopodia. Lpd's localization is independent of Ena/VASP proteins and free barbed ends of actin filaments. Furthermore, redistribution of the Lpd EVH1 binding sites to the surface of mitochondria resulted in substantial corecruitment of

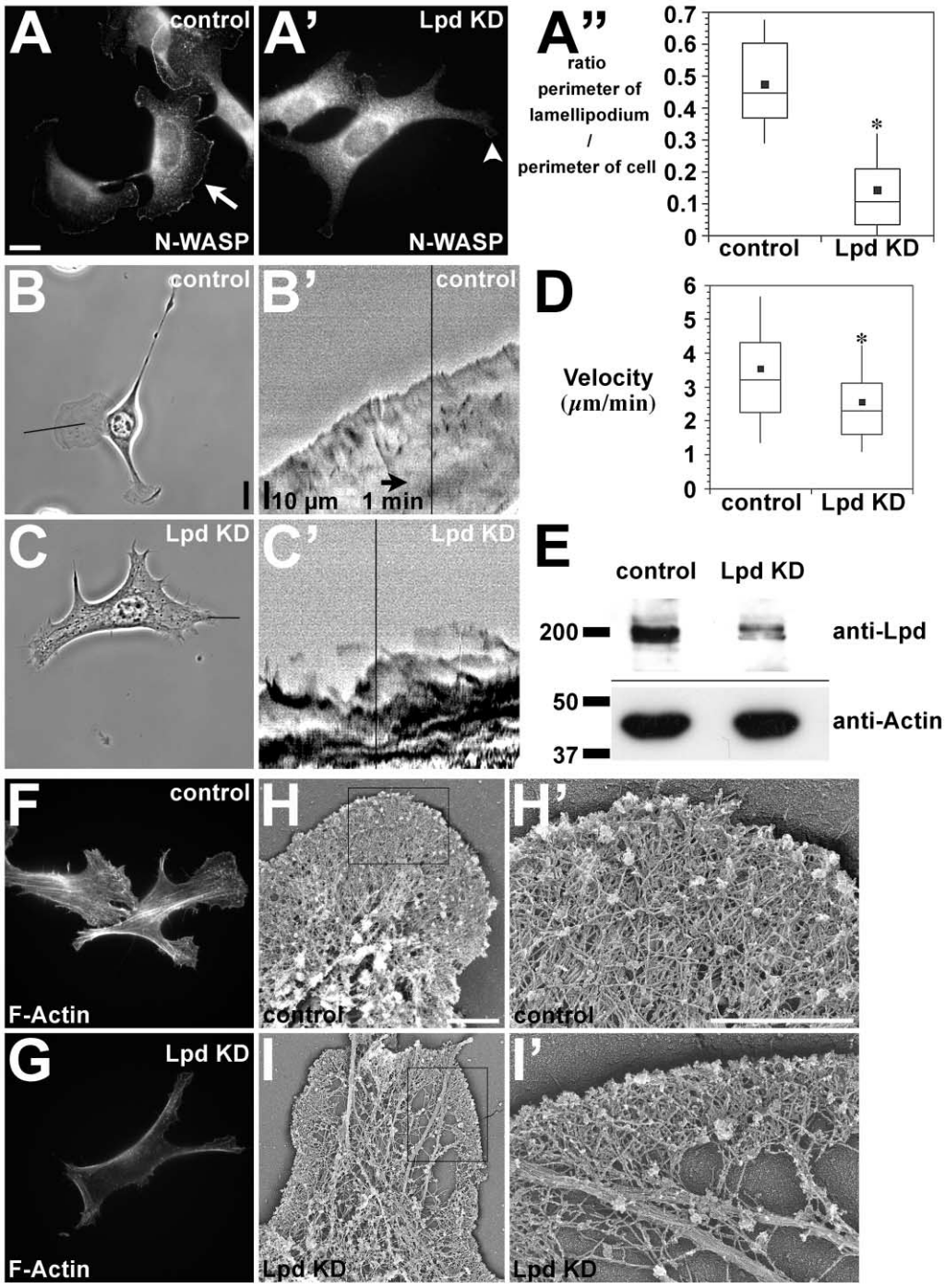

Figure 7. Knockdown of Lpd Expression Results in Impairment of Lamellipodia Formation

(A) B16-F1 cell lines stably expressing a control shRNA (A) or an shRNA against mouse Lpd (A′) were plated on laminin and fixed and stained with an N-WASP antibody (arrow in [A] and arrowhead indicating residual lamellipodia in [A′]). (A″) Quantification of the ratio of the length of lamellipodia to length of perimeter of cell depicted as box and whiskers plot (see Figure 6). Data is from 100 cells each. Nonoverlapping 95% convidence intervals are indicated by asterisks.

(B–D) Time-lapse movies of B16-F1 Lpd KD or control cells were analyzed by kymography (see Figure 6 for description of method). (D) Box and whisker plots for velocity of lamellipodial protrusion (t test, $p < 0.0001$, Lpd knockdown 172 and control 200 protrusion events). Nonoverlapping 95% convidence intervals are indicated by asterisks.

(E) Western blot analysis of B16-F1 Lpd knockdown and control cell line. The upper part of the blot was probed with an antibody to Lpd and the lower part with an antibody against Actin.

(F–I) Analysis of F-actin in B16-F1 control and Lpd knockdown cell lines. Cells were plated on laminin and fixed, and F-actin was stained with Alexa 647 phalloidin (F and G) or processed for platinum replica electron microscopy (H and I). Scale bar in (A) (for [A], [A′], [F], and [G]) equals 15 μm; scale bars in (B) (for [B] and [C] panels), (H) (for [H] and [I]), and (H′) (for [H′] and [I′]) represent 10 μm.

Ena/VASP. Therefore, Lpd may recruit and restrict Ena/VASP proteins to the tips of lamellipodia. It is, however, difficult to evaluate the role of Lpd in Ena/VASP recruitment to lamellipodia since Lpd depletion causes dramatic reduction in lamellipodial formation.

Similar to Lpd, the related protein RIAM (see accompanying article by Lafuente et al. [2004]), the mammalian unconventional cadherin Fat1 (Tanoue and Takeichi, 2004), and additional EVH1 ligands (M.K. and F.B.G., unpublished results) localize to the leading edge and may all function to recruit Ena/VASP proteins to these sites. It seems likely that EVH1-mediated interactions recruit Ena/VASP to different protein complexes within similar subcellular locations. For example, Ena/VASP-Fat1 complexes may be linked to adhesion signaling in lamellipodia, whereas Ena/VASP-Lpd/RIAM complexes would be linked to phosphoinositide and Ras superfamily signaling.

RIAM and Lpd Have Some Nonoverlapping Functions

The RA domain of RIAM interacts specifically with activated Rap1 (see accompanying article by Lafuente et al. [2004]). However, neither Lpd nor fragments of Lpd (RA-PH, RA) bind to Rap1 or other "classical" Ras GTPases (K-Ras, Rap2 RalA, and RalB) or to the Rho GTPases (Rho, Cdc42, and Rac) in biochemical protein-protein interaction or yeast two-hybrid assays (Supplemental Figure S1 at http://www.developmentalcell.com/cgi/content/full/7/4/571/DC1/). This suggests that the RA domains of Lpd and RIAM have different binding specificities. Therefore, in cells expressing both RIAM and Lpd, the two proteins may couple Ena/VASP to distinct sets of Ras superfamily proteins within lamellipodia.

RIAM and Lpd also exhibit opposing effects on cell adhesion. RIAM positively regulates adhesion. In Jurkat T cells, RIAM is required for Rap1 to stimulate integrin-mediated adhesion, potentially by recruiting activated Rap1 to the plasma membrane. This property of RIAM appears to be independent of Ena/VASP function. In contrast, Lpd negatively regulates adhesion (see accompanying article by Lafuente et al. [2004]). This is consistent with a model in which Lpd and RIAM can participate in independent signaling pathways and have some distinct functions due to differences in RA domain binding specificities.

A recent report analyzed the interaction of a set of Ras proteins with a panel of RA domain-containing proteins (Rodriguez-Viciana et al., 2004). The authors cotransfected GST fusions of activated Ras proteins with tagged RA domain-containing proteins and then analyzed GST pull-downs from cell lysates for the tagged protein by Western blotting. Using this approach, tagged Lpd-S could be detected in pull-down assays with GST fusions of activated K-Ras, N-Ras, H-Ras, and R-Ras-3 (Rodriguez-Viciana et al., 2004). We were unable to detect direct binding of Lpd to activated K-Ras by yeast two-hybrid or in vitro binding of the LPD-RA domain with purified K-Ras protein. There are at least two potential explanations for this apparent discrepancy. First, it is possible that tagged Lpd-S was pulled down indirectly (in a multiprotein complex) rather than by direct binding of Ras proteins to the Lpd RA domain. Second, it is possible that direct interaction of the Lpd RA domain with Ras proteins requires posttranslational modification (e.g., Ras farnyslation) and would have been missed in our assays. Further work will be required to determine which Ras proteins interact directly with Lpd in cells.

Lpd May Function as a Regulator of Lamellipodial Dynamics

Lpd knockdown leads to a reduction in lamellipodia perimeter, a reduction in velocity of residual lamellipodia, and a dramatic decrease in cellular F-actin content. This decrease in F-actin is evident in the large areas devoid of the dendritic arrays of actin filaments normally found within the cell periphery. These effects on lamellipodia formation and F-actin networks are more severe than those arising from loss of Ena/VASP function and suggest that Lpd signals to other important effectors of actin polymerization in addition to Ena/VASP. Interestingly, Lpd has been identified in protein complexes that also contain N-WASP, Scar/WAVE, and Mena (Salazar et al., 2003). Furthermore, Jurkat T cells in which RIAM has been knocked down exhibit dramatic reductions of F-actin content (see accompanying article by Lafuente et al. [2004]), suggesting that regulation of F-actin content may be a conserved function of both RIAM and Lpd.

Lamellipodin May Link PI-3 Kinase Signaling at the Leading Edge to Effectors of the Actin Cytoskeleton

Like many other important regulators of actin dynamics, Lpd localizes to the lamellipodial plasma membrane. The PH domain of Lpd is sufficient for leading edge targeting upon PDGF treatment of fibroblasts. This treatment is known to induce the production of 3′-phosphorylated phosphoinositides, PI(3,4)P_2 and PI(3,4,5)P_3 (Rameh and Cantley, 1999). Similarly, PI-3 kinases are asymmetrically recruited and activated at the leading edge when cells are exposed to gradients of chemotactic factors (Bourne and Weiner, 2002; Iijima et al., 2002; Merlot and Firtel, 2003).

The PH domain of Lpd binds specifically to PI(3,4)P_2. The only other known proteins that possess a PH domain specific for PI(3,4)P_2 are TAPP1 and TAPP2 (Dowler et al., 2000). Similar to our observation for Lpd, the PH domain of TAPP1 and TAPP2 is both necessary and sufficient for the plasma membrane targeting following PDGF treatment in fibroblasts (Kimber et al., 2002).

Most research into the role of 3′-phosphorylated phosphatidylinositides has employed the PH domain of Akt, which binds to both PI(3,4,5)P_3 and PI(3,4)P_2 (reviewed in Vanhaesebroeck et al., 2001); therefore, the precise role of PI(3,4)P_2 remains unclear. However, several reports have implicated PI(3,4)P_2 as one of the first asymmetric signals at the leading edge. The 5′-phosphatase SHIP-2 localizes to lamellipodia upon EGF treatment and catalyzes the degradation of PI(3,4,5)P_3 to PI(3,4)P_2 (Dyson et al., 2001). We suggest that Lpd, as a binding partner of both PI(3,4)P_2 and Ena/VASP proteins, provides a link between the initial asymmetric signal downstream of chemotaxis receptors and Ena/

VASP proteins as well as other regulators of actin polymerization.

Experimental Procedures

Molecular Cloning and Northern Blot Analysis

Subcloning and PCR were performed using standard methods. EST clones were purchased from Genome Systems/Incyte (Beverly, MA), and the cDNA of KIAA1681 was a gift of T. Nagase (Kazusa DNA Research Institute, Kisarazu, Chiba, Japan). Full-length human Lpd cDNA (AY494951) was obtained by amplifying the 5′ part of EST clone (IMAGE 2814736) and cloning it into the unique Bgl II site at the N terminus of the KIAA1681 cDNA. EGFP expression constructs were cloned by amplifying full-length Lpd, N-term-RAPH (aa 1–529), RAPH (aa 254–529), and PH (aa 383–547) fragments and cloning them into pML^2(EGFP-N1) and/or pEGFP-N1/C1. pML^2(EGFP-N1) was derived by subcloning EGFP and multiple cloning sites from pEGFP-N1 into pMSCVneo (Clontech). The Mito targeting constructs were made by cloning Lpd fragments aa 544–726 (Lpd-pro-Mito) and aa 888–1061 (Lpd-FP4-2-Mito) into a retroviral vector pBLT-2. The Lpd knockdown constructs were made by cloning Lpd-specific oligonucleotides (mouse Lpd: forward, 5′-tgcgtcaagtcacag aaccattcaagagatggttctgtgacttgacgctttttggaaagaattcg-3′; reverse, 5′-tcgacgaattctttccaaaaagcgtcaagtcacagaaccatctcttgaatggttctgt gacttgacgca-3′; rat Lpd: forward, 5′-TgcgccaagtcacagaacccTTCAA GAGAgggttctgtgacttggcgcTTTTTGGAAAGAATTCG-3′; reverse, 5′-tcgaCGAATTCTTTCCAAAAAgcgccaagtcacagaacccTCTCTTGAA gggttctgtgacttggcgcA-3′) into pLL3.7 and used to generate lentivirus as described (Rubinson et al., 2003). All constructs were verified by DNA sequencing.

The murine multiple tissue Northern blot (Ambion, Austin, TX) was probed with a Not I-Sac I, 520 bp, N-terminal fragment of the EST clone AW490888.

Proteins and Antibody Production

Fragments encoding amino acids aa 383–547 (Lpd-GST-PH), aa 726–888 (Lpd-GST-Fp4-1), aa 888–1060 (Lpd-GST-FP4-2), aa 1026–1126 (Lpd-GST-FP4-3), and aa 1126–1250 (Lpd-GST-FP4-4) were generated by PCR and cloned into the pGEX-6P1 vector (Amersham Pharmacia Biotech). Full-length cDNAs from Ras and Rho GTPases were amplified from EST clones and cloned into pGEX-6P1. GST-fusion proteins were purified on glutathione agarose (Pierce). Immobilized Lpd-GST-FP4-2 was digested with Prescission protease (Amersham Pharmacia Biotech) and used to raise polyclonal rabbit antiserum #3917 (Covance), which was affinity purified using cross-linked Lpd-GST-FP4-2 agarose.

Maltose binding protein fusion proteins were generated by amplifying RA domains of Lpd (aa 245–394) or c-Raf-1 (aa 26–175 = RIP3) (Vojtek et al., 1993) and cloning into pMAL-c2G (NEB) and were purified on Amylose resin following the instructions of the vendor (NEB). Purified, recombinant VASP was a gift of Melanie Barzik (MIT, Cambridge, MA).

Cell Culture and Fluorescence Microscopy

B16-F1 (ATCC CRL-6323), WI-38 (ATCC CCL-75), and Rat2 (ATCC CRL-1764) cells were cultured as recommended by ATCC. MV^{D7} cells were cultured as described (Bear et al., 2000). CAD cells were cultured as described (Qi et al., 1997). Retroviral packaging, infection, and fluorescence-activated cell sorting (FACS) was done as described (Loureiro et al., 2002). Lpd knockdown cell lines were obtained by infection with lentivirus expressing Lpd-specific shRNA and CMV promotor driven EGFP and sorted by FACS for high EGFP expression. Since cell population drifted extensively, cells were used for only two passages after the last FACS sort. Fugene (Roche) or standard calcium phosphate were used for transfection of CAD cells and 293, respectively. For immunofluorescence analysis, cells were plated on acid-washed coverslips coated with either 10 μg/ml fibronectin or 25 μg/ml laminin.

Primary hippocampal neurons were prepared from mouse embryos (day E16) as described for rat embryos (day E18) (Goslin and Banker, 1989). Glial cultures were prepared from P1 mouse cortex and hippocampus as described (Voutsinos-Porche et al., 2003). Hippocampal neurons were plated on poly-D-lysine-coated coverslips and maintained for 24–48 hr in glial-conditioned media (Neurobasal, 2% (v/v) B27 supplement, 1% (v/v) Glutamine (GIBCO-BRL).

Cell were fixed either with methanol for 10 min at −20°C or with 4% (w/v) paraformaldehyde in PHEM (60 mM PIPES, 25 mM HEPES, 10 mM EGTA, 2 mM $MgCl_2$, 120 mM sucrose, 4% (w/v) paraformaldehyde [pH 7.3]) for 20 min at room temperature and permeabilized with 0.1% (v/v) Triton-x-100 in TBS. The following antibodies were used: mAb anti Mena A351F7D9 (Lebrand et al., 2004), pAb anti-Lpd #3917, anti-N-WASP pAb (Rohatgi et al., 1999). Images were collected on either a Deltavision system (Applied Precision) or a Nikon TE2000 microscope equipped with a Yokagawa spinning disk confocal head (McBain Instruments) and an Orca-ER digital camera (Hamamatsu, Japan) and processed using Photoshop 7.0 (Adobe). CD treatment and kymography were performed as described (Bear et al., 2002).

Platinum Replica Electron Microscopy

Cells were plated on laminin-coated coverslips and processed for electron microscopy as described (Svitkina and Borisy, 1998).

Vaccinia Infection

HeLa cells were infected with the *Vaccinia* virus Western Reserve strain at a MOI of 1 pfu per cell in serum-free MEM for 1 hr at 37°C. Cells were incubated with MEM + 10% FCS for 8 hr and then fixed.

EPEC, *Listeria*, and *Shigella* Infections

HeLa cells in MEM + 10% FCS were infected with 20 μl of an overnight bacterial culture of *Entheropatogenic Escherichia coli (EPEC)* (strain E2348/69), *Shigella flexneri* (strain SC301), and *Listeria monocytogenes* (strain 10403S). After 4 hr the cells were fixed.

Protein Interaction Assays

SPOTS membranes (Sigma Genosys) were overlayed as described (Niebuhr et al., 1997) with purified recombinant EVL. Bound EVL was detected using monoclonal antibodies to EVL (#84H1) and the ECL kit (Amersham). Film was scanned and analyzed with ImageQuant (Molecular Dynamics).

Protein-lipid overlay and liposome binding assays were done as described (Kanai et al., 2001; Kavran et al., 1998). Ras and Rho GTPase in vitro binding studies were done as described (Vojtek et al., 1993).

F-Actin Measurement

F-actin was quantified as described (Diakonova et al., 2002). Briefly, 7×10^5 cells were plated per well on laminin-coated 6-well dishes. After 5 hr, cells were fixed and stained for 30 min in the dark with 250 nM rhodamine-phalloidin, 0.1% TritonX-100, 4% PFA in PHEM. After 3 washes with 5 ml PBS, cells were scraped off with 700 μl Methanol and extracted for 24 hr at −20°C. DNA content was measured from each sample by using PicoGreen (Molecular Probes) and used to normalize for variations in cell numbers. Extracted rhodamine-phalloidin was measured using a spectrofluometer (FluoroMax-3, Jobin Yvon, Inc.) (excitation 540 nm and emission 565 nm).

Immunoprecipitation and Western Blot Analysis

Neocortex was dissected from E16 mouse embryos and plated at 11×10^6 cells/dish on poly-D-lysine-coated 60 mm dishes. Neurons were cultured in Neurobasal, 2% (v/v) B27 supplement, 1% (v/v) Glutamine (GIBCO-BRL) for 48 hr and lysed with ice-cold GST-buffer (50 mM Tris-Cl, 200 mM NaCl, 1% (v/v) IGEPAL CA-630, 2 mM $MgCl_2$, 10% (v/v) glycerol [pH 7.4]), phosphatase inhibitors (1 mM Na_3VO_4, 10 mM NaF), and a protease inhibitor cocktail (Roche complete protease inhibitor tablets without EDTA). Lysates were incubated for 30 min on ice and centrifuged for 15 min at 18,000 × g at 4°C. Supernatants (700 μg/reaction) were precleared with protein-A agarose and immunoprecipitated with polyclonal antiserum #3917 against Lpd or preserum as control, and protein-A agarose (Pierce). After washing with GST-buffer, immunoprecipitated proteins were separated on 7.5% SDS-PAGE gels and transferred to Immobilon-P membranes (Millipore). Blots were probed with the anti-Mena mAb A351F7D9 and an HRP-coupled donkey anti-mouse secondary antibody (Jackson Immunologicals) and developed using the ECL kit (Amersham-Pharmacia Biotech).

Yeast Two-Hybrid Analysis

Full-length Ras and Rho GTPases were cloned into the "bait" vector pLexA (Clontech) and either full-length RIAM and Lpd or a fragment covering the RA-PH domains (aa 150–430 for RIAM, aa 245–529 for Lpd) were cloned into the "prey" vector pB42AD (Clontech). Plasmids were transformed into yeast strains EGY48 and EGY191 (Invitrogen). Transformants were plated on plates with selection media (SD/Gal/Raf/-His/-Trp/-Ura/-Leu) containing X-gal (20 μg/ml) for blue and white screening.

Acknowledgments

We thank T. Nagase (Kazusa DNA Research Institute, Kisarazu, Chiba, Japan) for cDNA of KIAA1681, R. Rohatgi and M. Kirschner (Harvard Medical School) for anti-N-WASP antibody, M. Barzik for purified VASP, Angelique Dousis for technical assistance, and Adam Kwiatkowski and Joe Loureiro for comments on the manuscript. Funding was provided by a Keck Distinguished Scholar award and NIH GM68678 to F.B.G. D.A.R. was supported by a Ludwig Fellowship.

Received: December 11, 2003
Revised: May 25, 2004
Accepted: July 19, 2004
Published: October 11, 2004

References

Ball, L.J., Kuhne, R., Hoffmann, B., Hafner, A., Schmieder, P., Volkmer-Engert, R., Hof, M., Wahl, M., Schneider-Mergener, J., Walter, U., et al. (2000). Dual epitope recognition by the VASP EVH1 domain modulates polyproline ligand specificity and binding affinity. EMBO J. *19*, 4903–4914.

Bashaw, G.J., Kidd, T., Murray, D., Pawson, T., and Goodman, C.S. (2000). Repulsive axon guidance: Abelson and Enabled play opposing roles downstream of the roundabout receptor. Cell *101*, 703–715.

Bear, J.E., Loureiro, J.J., Libova, I., Fassler, R., Wehland, J., and Gertler, F.B. (2000). Negative regulation of fibroblast motility by Ena/VASP proteins. Cell *101*, 717–728.

Bear, J.E., Svitkina, T.M., Krause, M., Schafer, D.A., Loureiro, J.J., Strasser, G.A., Maly, I.V., Chaga, O.Y., Cooper, J.A., Borisy, G.G., and Gertler, F.B. (2002). Antagonism between Ena/VASP proteins and actin filament capping regulates fibroblast motility. Cell *109*, 509–521.

Bourne, H.R., and Weiner, O. (2002). A chemical compass. Nature *419*, 21.

Celli, J., Deng, W., and Finlay, B.B. (2000). Enteropathogenic *Escherichia coli* (EPEC) attachment to epithelial cells: exploiting the host cell cytoskeleton from the outside. Cell. Microbiol. *2*, 1–9.

Chakraborty, T., Ebel, F., Domann, E., Niebuhr, K., Gerstel, B., Pistor, S., Temm-Grove, C.J., Jockusch, B.M., Reinhard, M., Walter, U., et al. (1995). A focal adhesion factor directly linking intracellularly motile *Listeria monocytogenes* and *Listeria ivanovii* to the actin-based cytoskeleton of mammalian cells. EMBO J. *14*, 1314–1321.

Cossart, P. (2000). Actin-based motility of pathogens: the Arp2/3 complex is a central player. Cell. Microbiol. *2*, 195–205.

Diakonova, M., Bokoch, G., and Swanson, J.A. (2002). Dynamics of cytoskeletal proteins during Fcgamma receptor-mediated phagocytosis in macrophages. Mol. Biol. Cell *13*, 402–411.

Dowler, S., Currie, R.A., Campbell, D.G., Deak, M., Kular, G., Downes, C.P., and Alessi, D.R. (2000). Identification of pleckstrin-homology-domain-containing proteins with novel phosphoinositide-binding specificities. Biochem. J. *351*, 19–31.

Dowler, S., Kular, G., and Alessi, D.R. (2002). Protein lipid overlay assay. Sci STKE *2002*, PL6.

Drees, B., Friederich, E., Fradelizi, J., Louvard, D., Beckerle, M.C., and Golsteyn, R.M. (2000). Characterization of the interaction between zyxin and members of the Ena/vasodilator-stimulated phosphoprotein family of proteins. J. Biol. Chem. *275*, 22503–22511.

Dyson, J.M., O'Malley, C.J., Becanovic, J., Munday, A.D., Berndt, M.C., Coghill, I.D., Nandurkar, H.H., Ooms, L.M., and Mitchell, C.A. (2001). The SH2-containing inositol polyphosphate 5-phosphatase, SHIP-2, binds filamin and regulates submembraneous actin. J. Cell Biol. *155*, 1065–1079.

Frischknecht, F., and Way, M. (2001). Surfing pathogens and the lessons learned for actin polymerization. Trends Cell Biol. *11*, 30–38.

Fruman, D.A., Rameh, L.E., and Cantley, L.C. (1999). Phosphoinositide binding domains: embracing 3-phosphate. Cell *97*, 817–820.

Gertler, F.B., Niebuhr, K., Reinhard, M., Wehland, J., and Soriano, P. (1996). Mena, a relative of VASP and *Drosophila* Enabled, is implicated in the control of microfilament dynamics. Cell *87*, 227–239.

Goslin, K., and Banker, G. (1989). Experimental observations on the development of polarity by hippocampal neurons in culture. J. Cell Biol. *108*, 1507–1516.

Gruenheid, S., and Finlay, B.B. (2003). Microbial pathogenesis and cytoskeletal function. Nature *422*, 775–781.

Hadano, S., Hand, C.K., Osuga, H., Yanagisawa, Y., Otomo, A., Devon, R.S., Miyamoto, N., Showguchi-Miyata, J., Okada, Y., Singaraja, R., et al. (2001). A gene encoding a putative GTPase regulator is mutated in familial amyotrophic lateral sclerosis 2. Nat. Genet. *29*, 166–173.

Hinz, B., Alt, W., Johnen, C., Herzog, V., and Kaiser, H.W. (1999). Quantifying lamella dynamics of cultured cells by SACED, a new computer-assisted motion analysis. Exp. Cell Res. *251*, 234–243.

Iijima, M., Huang, Y.E., and Devreotes, P. (2002). Temporal and spatial regulation of chemotaxis. Dev. Cell *3*, 469–478.

Kanai, F., Liu, H., Field, S.J., Akbary, H., Matsuo, T., Brown, G.E., Cantley, L.C., and Yaffe, M.B. (2001). The PX domains of p47phox and p40phox bind to lipid products of PI(3)K. Nat. Cell Biol. *3*, 675–678.

Kavran, J.M., Klein, D.E., Lee, A., Falasca, M., Isakoff, S.J., Skolnik, E.Y., and Lemmon, M.A. (1998). Specificity and promiscuity in phosphoinositide binding by pleckstrin homology domains. J. Biol. Chem. *273*, 30497–30508.

Kimber, W.A., Trinkle-Mulcahy, L., Cheung, P.C., Deak, M., Marsden, L.J., Kieloch, A., Watt, S., Javier, R.T., Gray, A., Downes, C.P., et al. (2002). Evidence that the tandem-pleckstrin-homology-domain-containing protein TAPP1 interacts with Ptd(3,4)P2 and the multi-PDZ-domain-containing protein MUPP1 in vivo. Biochem. J. *361*, 525–536.

Krause, M., Sechi, A.S., Konradt, M., Monner, D., Gertler, F.B., and Wehland, J. (2000). Fyn-binding protein (Fyb)/SLP-76-associated protein (SLAP), Ena/vasodilator-stimulated phosphoprotein (VASP) proteins and the Arp2/3 complex link T cell receptor (TCR) signaling to the actin cytoskeleton. J. Cell Biol. *149*, 181–194.

Krause, M., Dent, E.W., Bear, J.E., Loureiro, J.J., and Gertler, F.B. (2003). ENA/VASP proteins: regulators of the actin cytoskeleton and cell migration. Annu. Rev. Cell Dev. Biol. *19*, 541–564.

Lafuente, E.M., van Puijenbroek, A.A.F.L., Krause, M., Carman, C.V., Freeman, G.J., Berezovskaya, A., Constantine, E., Springer, T.A., Gertler, F.B., and Boussiotis, V.A. (2004). RIAM, an Ena/VASP and profilin ligand, interacts with Rap1-GTP and mediates Rap1-induced adhesion. Dev. Cell *7*, this issue, 585–595.

Lanier, L.M., Gates, M.A., Witke, W., Menzies, A.S., Wehman, A.M., Macklis, J.D., Kwiatkowski, D., Soriano, P., and Gertler, F.B. (1999). Mena is required for neurulation and commissure formation. Neuron *22*, 313–325.

Lebrand, C., Dent, E.W., Strasser, G.A., Lanier, L.M., Krause, M., Svitkina, T.M., Borisy, G.G., and Gertler, F.B. (2004). Critical role of Ena/VASP proteins for filopodia formation in neurons and in function downstream of Netrin-1. Neuron *42*, 37–49.

Loureiro, J.J., Rubinson, D.A., Bear, J.E., Baltus, G.A., Kwiatkowski, A.V., and Gertler, F.B. (2002). Critical roles of phosphorylation and actin binding motifs, but not the central proline-rich region, for Ena/vasodilator-stimulated phosphoprotein (VASP) function during cell migration. Mol. Biol. Cell *13*, 2533–2546.

Manser, J., Roonprapunt, C., and Margolis, B. (1997). *C. elegans* cell migration gene mig-10 shares similarities with a family of SH2 domain proteins and acts cell nonautonomously in excretory canal development. Dev. Biol. *184*, 150–164.

Merlot, S., and Firtel, R.A. (2003). Leading the way: directional sensing through phosphatidylinositol 3-kinase and other signaling pathways. J. Cell Sci. *116*, 3471–3478.

Niebuhr, K., Ebel, F., Frank, R., Reinhard, M., Domann, E., Carl, U.D., Walter, U., Gertler, F.B., Wehland, J., and Chakraborty, T. (1997). A novel proline-rich motif present in ActA of *Listeria monocytogenes* and cytoskeletal proteins is the ligand for the EVH1 domain, a protein module present in the Ena/VASP family. EMBO J. *16*, 5433–5444.

Qi, Y., Wang, J.K., McMillian, M., and Chikaraishi, D.M. (1997). Characterization of a CNS cell line, CAD, in which morphological differentiation is initiated by serum deprivation. J. Neurosci. *17*, 1217–1225.

Rameh, L.E., and Cantley, L.C. (1999). The role of phosphoinositide 3-kinase lipid products in cell function. J. Biol. Chem. *274*, 8347–8350.

Reinhard, M., Halbrugge, M., Scheer, U., Wiegand, C., Jockusch, B.M., and Walter, U. (1992). The 46/50 kDa phosphoprotein VASP purified from human platelets is a novel protein associated with actin filaments and focal contacts. EMBO J. *11*, 2063–2070.

Rietdorf, J., Ploubidou, A., Reckmann, I., Holmstrom, A., Frischknecht, F., Zettl, M., Zimmermann, T., and Way, M. (2001). Kinesin-dependent movement on microtubules precedes actin-based motility of vaccinia virus. Nat. Cell Biol. *3*, 992–1000.

Rodriguez-Viciana, P., Sabatier, C., and McCormick, F. (2004). Signaling specificity by ras family GTPases is determined by the full spectrum of effectors they regulate. Mol. Cell. Biol. *24*, 4943–4954.

Rohatgi, R., Ma, L., Miki, H., Lopez, M., Kirchhausen, T., Takenawa, T., and Kirschner, M.W. (1999). The interaction between N-WASP and the Arp2/3 complex links Cdc42-dependent signals to actin assembly. Cell *97*, 221–231.

Rottner, K., Behrendt, B., Small, J.V., and Wehland, J. (1999). VASP dynamics during lamellipodia protrusion. Nat. Cell Biol. *1*, 321–322.

Rubinson, D.A., Dillon, C.P., Kwiatkowski, A.V., Sievers, C., Yang, L., Kopinja, J., Rooney, D.L., Ihrig, M.M., McManus, M.T., Gertler, F.B., et al. (2003). A lentivirus-based system to functionally silence genes in primary mammalian cells, stem cells and transgenic mice by RNA interference. Nat. Genet. *33*, 401–406.

Salazar, M.A., Kwiatkowski, A.V., Pellegrini, L., Cestra, G., Butler, M.H., Rossman, K.L., Serna, D.M., Sondek, J., Gertler, F.B., and De Camilli, P. (2003). Tuba: a novel protein containing Bin/Amphiphysin/Rvs (BAR) and Dbl homology domains links dynamin to regulation of the actin cytoskeleton. J. Biol. Chem. *278*, 49031–49043.

Servant, G., Weiner, O.D., Neptune, E.R., Sedat, J.W., and Bourne, H.R. (1999). Dynamics of a chemoattractant receptor in living neutrophils during chemotaxis. Mol. Biol. Cell *10*, 1163–1178.

Servant, G., Weiner, O.D., Herzmark, P., Balla, T., Sedat, J.W., and Bourne, H.R. (2000). Polarization of chemoattractant receptor signaling during neutrophil chemotaxis. Science *287*, 1037–1040.

Smith, G.L., Vanderplasschen, A., and Law, M. (2002). The formation and function of extracellular enveloped vaccinia virus. J. Gen. Virol. *83*, 2915–2931.

Svitkina, T.M., and Borisy, G.G. (1998). Correlative light and electron microscopy of the cytoskeleton of cultured cells. Methods Enzymol. *298*, 570–592.

Svitkina, T.M., Neyfakh, A.A., Jr., and Bershadsky, A.D. (1986). Actin cytoskeleton of spread fibroblasts appears to assemble at the cell edges. J. Cell Sci. *82*, 235–248.

Tanoue, T., and Takeichi, M. (2004). Mammalian Fat1 cadherin regulates actin dynamics and cell-cell contact. J. Cell Biol. *165*, 517–528.

Vanhaesebroeck, B., Leevers, S.J., Ahmadi, K., Timms, J., Katso, R., Driscoll, P.C., Woscholski, R., Parker, P.J., and Waterfield, M.D. (2001). Synthesis and function of 3-phosphorylated inositol lipids. Annu. Rev. Biochem. *70*, 535–602.

Vojtek, A.B., Hollenberg, S.M., and Cooper, J.A. (1993). Mammalian Ras interacts directly with the serine/threonine kinase Raf. Cell *74*, 205–214.

Voutsinos-Porche, B., Bonvento, G., Tanaka, K., Steiner, P., Welker, E., Chatton, J.Y., Magistretti, P.J., and Pellerin, L. (2003). Glial glutamate transporters mediate a functional metabolic crosstalk between neurons and astrocytes in the mouse developing cortex. Neuron *37*, 275–286.